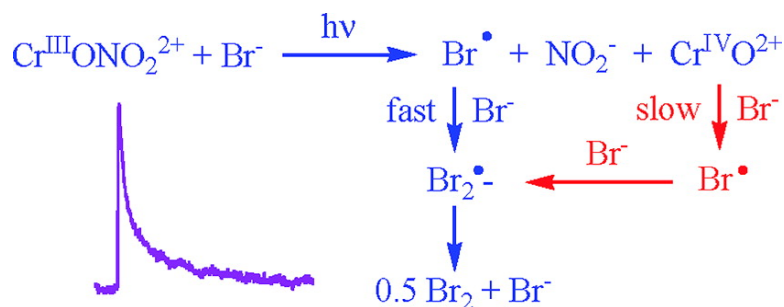


Photochemical Oxidation of Halide Ions by a Nitratochromium(III) Complex. Kinetics, Mechanism, and Intermediates

Mingming Cheng, and Andreja Bakac

J. Am. Chem. Soc., **2008**, 130 (16), 5600-5605 • DOI: 10.1021/ja8000453 • Publication Date (Web): 01 April 2008

Downloaded from <http://pubs.acs.org> on February 8, 2009



More About This Article

Additional resources and features associated with this article are available within the HTML version:

- Supporting Information
- Links to the 1 articles that cite this article, as of the time of this article download
- Access to high resolution figures
- Links to articles and content related to this article
- Copyright permission to reproduce figures and/or text from this article

[View the Full Text HTML](#)



ACS Publications
 High quality. High impact.

Photochemical Oxidation of Halide Ions by a Nitratochromium(III) Complex. Kinetics, Mechanism, and Intermediates

Mingming Cheng and Andreja Bakac*

Department of Chemistry, Iowa State University, Ames, Iowa 50011

Received January 8, 2008; E-mail: bakac@iastate.edu

Abstract: The 266 nm laser flash photolysis of the title complex in the presence of halide ions X^- ($X = I, Br, \text{ and } Cl$) generates halogen atoms on nanosecond time scales, followed by the known X^*/X^- reactions to yield dihalide radical anions, $X_2^{\bullet-}$. Plots of k_{obs} against the concentration of X^- were linear with zero intercepts, but the yields of $X_2^{\bullet-}$ increased with increasing concentrations of $[X^-]$. This result suggests that a short-lived, strongly oxidizing intermediate reacts with X^- to generate X^* in parallel with the decomposition to $Cr_{\text{aq}}O^{2+}$ and $\bullet NO_2$, both of which were identified in steady-state photolysis experiments in the presence of selective trapping agents. Bromide was oxidized quantitatively to bromine, and a combination of molecular oxygen and methanol channeled the reaction toward superoxochromium(III) ion, $Cr_{\text{aq}}OO^{2+}$. In the absence of scavengers, nitrite and chromate were produced. The proposed reaction scheme draws additional support from the good agreement between the experimental product yields and those predicted by kinetic simulations.

Introduction

Nitrate anion is widespread in Nature. It is an essential nutrient for plants, an important component in aqueous atmospheric chemistry, including acid rain, and a major contaminant in ground waters. Thermal reduction of nitrate in biological environments is catalyzed by nitrate reductases, which are currently the subject of intense structural and mechanistic studies.^{1–4} Photochemical reduction generates nitrite and O_2 by a reasonably well-understood mechanism^{5–7} involving mainly peroxyxynitrite (48%) and either $\{\bullet NO + O_2^{\bullet-}\}$ or $\{NO^- + O_2\}$ (8%) as intermediates, while 44% of the excited state deactivates to the ground state NO_3^- .

The photochemistry of nitrate metal complexes is much less explored. In one example, UV irradiation of $(PPh_3)_2Cu^I NO_3$ in acetonitrile led to the oxidation of PPh_3 and formation of NO .⁸ The intraligand (PPh_3) excited state was proposed to relax to the $Cu(I)$ -to- NO_3^- MLCT state leading to N–O bond cleavage and formation of $(PPh_3)_2Cu^{II}O$ and $\bullet NO_2$.⁸ A rapid follow-up reaction between $\bullet NO_2$ and PPh_3 completed the sequence. The photolysis of a nitrate complex of a manganese(III) porphyrin was reported to generate a manganese(IV) oxo species that was able to oxidize styrene and PPh_3 .⁹ A related nitrateiron(III)

complex also engaged in photochemical oxidations, including hydroxylation of C–H bonds, which has led the authors to propose $O=Fe^{IV}(TPP^{\bullet+})$ ($TPP = \text{tetraphenylporphyrin}$) as a reaction intermediate and active oxidant.⁹ In this case, all three oxygens of the coordinated nitrate were involved in substrate oxidation.

In the present work, we have explored the photochemical reactivity of a nitrate complex of chromium(III), $(H_2O)_5-CrONO_2^{2+}$. Despite the vast amount of literature data on the photochemistry and photophysics of chromium(III) complexes,^{10–13} there are only a handful of examples of redox photochemistry^{14–17} for complexes with simple nonparticipating ligands, such as water or amines. Instead, aquation, ligand exchange, racemization, etc. dominate. Chromium(III) polypyridine complexes, on the other hand, turn into powerful oxidants upon excitation with visible light.¹⁸

The main reason for the marginal role of redox chemistry is undoubtedly the low reduction potential of $Cr(II)$ which favors back-electron transfer in both the solvent cage and bulk solution to regenerate the reactants or perhaps induce ligand substitution.¹¹ The photochemistry of $(NH_3)_5CrBr^{2+}$ and related complexes illustrates the point.¹⁴ Flash photolysis at $\lambda \geq 300 \text{ nm}$

- (1) Tischner, R. J. *Crop Improvement* **2005**, *15*, 53–95.
- (2) Hofmann, M. J. *Biol. Inorg. Chem.* **2007**, *12*, 989–1001.
- (3) Fischer, K.; Barbier, G. G.; Hecht, H.-J.; Mendel, R. R.; Campbell, W. H.; Schwarz, G. *Plant Cell* **2005**, *17*, 1167–1179.
- (4) Ferguson, S. J.; Richardson, D. J. *Adv. Photosynth. Respiration* **2004**, *16*, 169–206.
- (5) Madsen, D.; Larsen, J.; Jensen, S. K.; Keiding, S. R.; Thogersen, J. *J. Am. Chem. Soc.* **2003**, *125*, 15571–15576.
- (6) Mark, G.; Korth, H.-G.; Schuchmann, H.-P.; Von Sonntag, C. J. *Photochem. Photobiol. A* **1996**, *101*, 89–103.
- (7) Vione, D.; Maurino, V.; Minero, C.; Pelizzetti, E.; Harrison, M. A. J.; Olariu, R.-I.; Arsene, C. *Chem. Soc. Rev.* **2006**, *35*, 441–453.
- (8) Kunkely, H.; Vogler, A. *J. Am. Chem. Soc.* **1995**, *117*, 540–541.
- (9) Suslick, K. S.; Watson, R. A. *Inorg. Chem.* **1991**, *30*, 912–919.

- (10) Zinato, E. In *Concepts of Inorganic Photochemistry*; Adamson, A. W., Fleischauer, P. D., Eds.; Wiley: New York, 1975; p 143–201.
- (11) Kirk, A. D. *Chem. Rev.* **1999**, *99*, 1607–1640.
- (12) Forster, L. S. *Chem. Rev.* **1990**, *90*, 331–353.
- (13) Endicott, J. F.; Ramasami, T.; Tamilarasan, R.; Lessard, R. B.; Ryu, C. K. *Coord. Chem. Rev.* **1987**, *77*, 1–87.
- (14) Sriram, R.; Endicott, J. F. *J. Chem. Soc., Chem. Commun.* **1976**, 683–684.
- (15) Bakac, A.; Espenson, J. H. *J. Chem. Soc., Chem. Commun.* **1990**, 1646–1647.
- (16) Vogler, A. *J. Am. Chem. Soc.* **1971**, *93*, 5912–5913.
- (17) Ruminski, R. R.; Healy, M. H.; Coleman, W. F. *Inorg. Chem.* **1989**, *28*, 1666–1669.
- (18) Balzani, V.; Bolletta, F.; Gandolfi, M. T.; Maestri, M. *Top. Curr. Chem.* **1978**, *75*, 1–64.

in the presence of free Br^- generates $\text{Br}_2^{\bullet-}$, which was detected on short time scales, but such solutions exhibited no reducing properties after photolysis. Obviously, the Cr(II) that was generated in the flash had recombined with $\text{Br}^\bullet/\text{Br}_2^{\bullet-}$ to regenerate chromium(III). This behavior stands in sharp contrast with that of the analogous cobalt complex, even though the initial photochemical event is believed to be similar, that is, Br^\bullet and $\text{Co}(\text{NH}_3)_5^{2+}$ are formed. In this case, however, the labile Co(II) product rapidly aquates to an extremely weak reductant, $\text{Co}_{\text{aq}}^{2+}$, and no back reaction takes place.

In general, the photochemistry of aqua complexes of Cr(III) has received much less attention than that of the ammine counterparts, perhaps because studies of the latter compounds provide more detailed information about the (predominant) substitution reactions. The lifetimes of the emitting ${}^2\text{E}$ states for the two parent complexes, $\text{Cr}(\text{NH}_3)_6^{3+}$ and $\text{Cr}(\text{H}_2\text{O})_6^{3+}$, differ by about 3 orders of magnitude. This has led to a suggestion that the shorter-lived ${}^* \text{Cr}(\text{H}_2\text{O})_6^{3+}$ ($\tau_0 = 2$ ns at 25 °C)¹⁹ perhaps decays by back intersystem crossing. Data are not available for the lifetimes of charge transfer excited states of substituted complexes, but we have in the past observed some reductive photochemistry with $\text{Cr}_{\text{aq}}\text{OO}^{2+}$,²⁰ $\text{Cr}_{\text{aq}}\text{NO}^{2+}$,²¹ and $\text{Cr}_{\text{aq}}\text{R}^{2+}$ (R = alkyl),²² all of which generate $\text{Cr}_{\text{aq}}^{2+}$ and oxidized ligand (O_2 , NO , or R^\bullet) upon UV photolysis, similar to the related ammine complexes such as $(\text{NH}_3)_5\text{CrBr}^{2+}$.¹⁴

Nitrate is a much poorer reductant⁸ than any of the active ligands in the above examples, which may channel the photochemistry of $(\text{H}_2\text{O})_5\text{CrONO}_2^{2+}$ in a different direction. The purpose of this study was to establish whether the photolysis of $(\text{H}_2\text{O})_5\text{CrONO}_2^{2+}$ results in productive photochemistry, to determine the reaction products, and to attempt to detect reaction intermediates as our contribution to the currently limited understanding of electron-transfer photochemistry of both coordinated nitrate and aquachromium(III) ions. Our results are also pertinent to aqueous atmospheric photochemistry where nitrate, nitrite, and halo metal complexes are likely to be involved as transients.

Experimental Section

Acidic aqueous solutions of $(\text{H}_2\text{O})_5\text{CrONO}_2^{2+}$ were prepared from molten $\text{Cr}(\text{NO}_3)_3 \cdot 9\text{H}_2\text{O}$ (Aldrich) at 100 °C according to a literature procedure.²³ The 2+ charged product was separated from $\text{Cr}_{\text{aq}}^{3+}$ and more highly charged dinuclear species on a column of ice-cold Dowex 50W-X8 cation exchange resin and eluted with 1.0 M HClO_4 . The stock solutions typically contained 40 mM $(\text{H}_2\text{O})_5\text{CrONO}_2^{2+}$, as determined from the UV-visible spectra.²³ Except when in use, these solutions were kept in a freezer where they remained unchanged for up to two months. Perchloric acid, NaCl, NaBr, and NaI were commercial products (Fisher) of the highest purity available and were used as received.

The kinetics of the formation and decay of $\text{X}_2^{\bullet-}$ radicals were monitored at their near-UV maxima at 330 nm (X = Cl), 360 (Br), and 380 (I). Pseudo-first-order rate constants for the formation of $\text{X}_2^{\bullet-}$ were obtained by fitting the experimental traces to eq 1, where Abs_t , Abs_{inf} , and Abs_0 represent absorbances at times t , at the end of the reaction, and at zero time.

$$\text{Abs}_t = \text{Abs}_{\text{inf}} + (\text{Abs}_{\text{inf}} - \text{Abs}_0)e^{-kt} \quad (1)$$

(19) Linck, N. J.; Berens, S. J.; Magde, D.; Linck, R. G. *J. Phys. Chem.* **1983**, *87*, 1733–1737.

(20) Bakac, A.; Scott, S. L.; Espenson, J. H.; Rodgers, K. L. *J. Am. Chem. Soc.* **1995**, *117*, 6483–6488.

(21) Nemes, A.; Pestovsky, O.; Bakac, A. *J. Am. Chem. Soc.* **2002**, *124*, 421–427.

(22) Bakac, A.; Espenson, J. H. *Inorg. Chem.* **1983**, *22*, 779–783.

(23) Swaddle, T. W. *J. Am. Chem. Soc.* **1967**, *89*, 4338–4344.

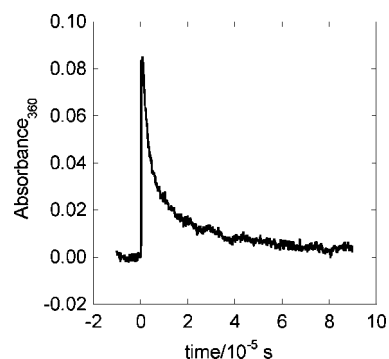


Figure 1. Kinetic trace for the growth and decay of $\text{Br}_2^{\bullet-}$ at 360 nm following a 266 nm laser flash of a solution containing 3.8 mM $(\text{H}_2\text{O})_5\text{CrONO}_2^{2+}$ and 20 mM Br^- in 0.16 M HClO_4 . Effective path length = 3 mm.

The rate constants for second-order decay of dihalide radical anions were obtained by fitting the data to the rate law of eq 2. The initial concentrations of $\text{X}_2^{\bullet-}$ were calculated from the initial absorbance, known molar absorptivities of $\text{X}_2^{\bullet-}$,²⁴ and an effective path length (equal to the diameter of the laser beam) of 3 mm.

$$\text{Abs}_t = \text{Abs}_{\text{inf}} + (\text{Abs}_0 - \text{Abs}_{\text{inf}})/(1 + 2kt[\text{X}_2^{\bullet-}]_0) \quad (2)$$

UV-vis spectral and kinetic measurements were done with a Shimadzu 3101 PC spectrophotometer. Laser flash photolysis experiments utilized the fourth harmonic of a Nd:Yag laser ($\lambda_{\text{exc}} = 266$ nm) and an LKS 50 Applied Photophysics laser flash photolysis instrument.²⁵ Steady-state photolyses were carried out in a Rayonet reactor, $\lambda_{\text{exc}} = 254$ nm.

In-house distilled water was further purified by passage through a Barnstead EASYpure III system. All the kinetic data were obtained at 25.0 ± 0.2 °C. Simulations utilized the program Chemical Kinetics Simulator (IBM).

Results

Laser Flash Photolysis. Flashing acidic, argon-saturated aqueous solutions containing 3.8 mM $(\text{H}_2\text{O})_5\text{CrONO}_2^{2+}$ ($\epsilon_{266} = 100 \text{ M}^{-1} \text{ cm}^{-1}$) caused a small increase in the UV absorbance around 260–270 nm, $\Delta\text{Abs} \sim 0.002$. Owing to the small absorbance change, it was not possible to determine the precise spectrum of the intermediate responsible, but the observed signal is consistent with the formation of $\sim 40 \mu\text{M}$ NO_2 ($\epsilon_{270} = 250 \text{ M}^{-1} \text{ cm}^{-1}$).²⁴ As shown below, this is in accord with other findings in our work.

Reaction with Halide Ions. No changes were observed in the UV-vis spectrum ($\lambda > 265$ nm) of $(\text{H}_2\text{O})_5\text{CrONO}_2^{2+}$ upon addition of up to 40 mM chloride or bromide. Iodide (≤ 10 mM) caused a small increase in absorbance, ϵ_{266} for $\text{I}^- = 7 \text{ M}^{-1} \text{ cm}^{-1}$. At shorter wavelengths, where halide ions also absorb, the observed spectrum was the sum of the spectra of $(\text{H}_2\text{O})_5\text{CrONO}_2^{2+}$ and X^- , with no evidence for ion pairs.

Laser flash photolysis of such solutions caused a rapid increase in absorbance followed by a slower decrease, with the greatest absorbance change taking place at the UV maxima of dihalide radical anions $\text{X}_2^{\bullet-}$, X = Cl, Br, or I, as shown for a reaction with 20 mM Br^- in Figure 1. The absorbance changes obtained with bromide and iodide were about 5–10 times larger than that for chloride which had ΔAbs_{330} of only 0.008 at 50

(24) Hug, G. L. *Optical Spectra of Nonmetallic Inorganic Transient Species in Aqueous Solution*; Radiation Chemistry Data Center, Radiation Laboratory, University of Notre Dame, 1981.

(25) Huston, P.; Espenson, J. H.; Bakac, A. *J. Am. Chem. Soc.* **1992**, *114*, 9510–9516.

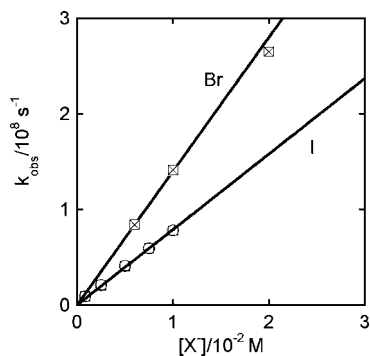


Figure 2. Plot of k_{obs} versus the concentration of halide ions for the formation of X_2^{*-} ($X = \text{Br}, \text{I}$) following the 266 nm flash. Conditions: $[(\text{H}_2\text{O})_5\text{CrONO}_2^{2+}] = 3.8 \text{ mM}$, $[\text{H}^+] = 0.16 \text{ M}$.

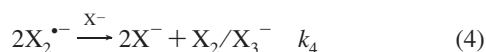
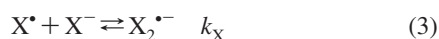
Table 1. Summary of Rate Constants for the Formation and Decay of X_2^{*-} ^a

X	$k_f/10^9 \text{ M}^{-1} \text{ s}^{-1b}$	$k_d/10^9 \text{ M}^{-1} \text{ s}^{-1c}$
Br	14.0 ± 0.2	4.0 ± 0.8
I	7.92 ± 0.10	23 ± 3

^a Generated by photolysis of $(\text{H}_2\text{O})_5\text{CrONO}_2^{2+}$ and halide ions (X^-) in 0.16 M HClO_4 . ^b Rate constant for reaction 3. ^c Rate constant for X_2^{*-} disproportionation.

mM Cl^- . The weak signal ruled out precise kinetic determinations for the chloride reaction, but the reaction time scale was comparable to that for other halides. The complex $(\text{H}_2\text{O})_5\text{CrONO}_2^{2+}$ was essential for all the observed photochemistry. No X_2^{*-} was observed in control experiments in the absence of $(\text{H}_2\text{O})_5\text{CrONO}_2^{2+}$, or with mixtures of X^- , $\text{Cr}_{\text{aq}}^{3+}$, and free NO_3^- .

The plots of k_{obs} against the concentration of halide ions for the formation of Br_2^{*-} and I_2^{*-} following the flash are linear and exhibit no measurable intercepts (Figure 2). The slopes of the straight lines yielded the rate constants $k_X = (1.40 \pm 0.02) \times 10^{10} \text{ M}^{-1} \text{ s}^{-1}$ (Br) and $(7.90 \pm 0.12) \times 10^9 \text{ M}^{-1} \text{ s}^{-1}$ (I), both of which are within the range of published rate constants²⁶ for the reaction between X^* and X^- to give X_2^{*-} (eq 3). The subsequent decay of X_2^{*-} followed second-order kinetics with rate constants that were somewhat greater than those reported for the bimolecular decay of X_2^{*-} ²⁶ (Table 1). Experiments with iodide, where both X_2^{*-} and the final product I_3^- absorb strongly at 380 nm, confirmed that precisely 0.5 equiv of I_3^- was produced per mole of I_2^{*-} reacting. We are thus confident that the observed second-order reaction is the disproportionation of the radical anions (eq 4).



Unexpectedly, the absorbance change for the growth of X_2^{*-} increased with the concentration of halide ions (Figure 3) and approached saturation at high $[X^-]$ as illustrated by the plot of absorbance versus $[X^-]$ in Figure 4. Given that molar absorptivities of I_2^{*-} and Br_2^{*-} at their respective maxima are within a few percent of each other, the absorbance data for the two halides are directly comparable. All the points fall reasonably

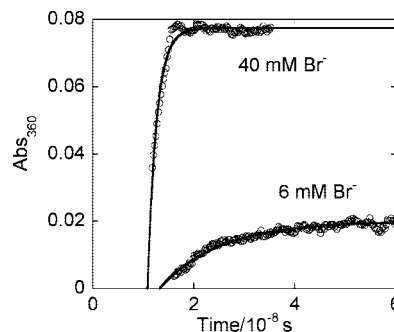


Figure 3. Kinetic traces at 360 nm for the formation of Br_2^{*-} at two different concentrations of bromide ions.

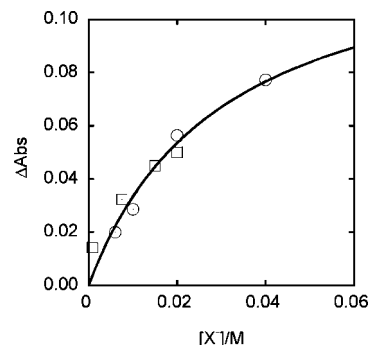


Figure 4. Plot of the absorbance increase for the growth of Br_2^{*-} (360 nm, circles) and I_2^{*-} (380 nm, squares) against the concentration of the respective halide ions. The line is a fit to eq 5.

well on a single curve described by eq 5, and yield $a = 0.13 \pm 0.03$ and $b = 0.03 \pm 0.01 \text{ M}$.

$$\text{Abs} = a/(1 + b/[X^-]) \quad (5)$$

At $[X^-] < 0.1 \text{ mM}$, the signal was too weak to observe. We will return to this point later but should note here that the equilibrium constants for the formation of X_2^{*-} (eq 3) are on the order of $2 \times 10^5 \text{ M}^{-1}$ for both dihalide radical anions.²⁶ Thus even at 0.1 mM X^- , more than 90% of X^* would be converted to X_2^{*-} . The fact that no observable signal remained shows that X^* was not produced at such low concentrations of halide ions.

Steady-State Photolysis. A 17 min UV photolysis ($\lambda 254 \text{ nm}$) of an argon-saturated solution containing 3.0 mM $(\text{H}_2\text{O})_5\text{CrONO}_2^{2+}$ in 0.10 M HClO_4 resulted in the formation of a broad maximum at $\sim 350 \text{ nm}$, corresponding to HCrO_4^- , and several small peaks in the 330–390 nm range, characteristic of HNO_2 . The yield of nitrite was determined in the reaction with iodide ions. For this determination, the irradiation time was reduced to 60 s to minimize secondary photolysis of reaction products, and sodium iodide was injected (final concentration = 0.60 mM). A two-step reaction was observed at the 350 nm maximum of I_3^- . The kinetics of the first step under both argon and oxygen were within a few percent of those reported in the literature,²⁷ and confirmed in independent experiments in this work, for the HNO_2/I^- reaction. From the absorbance change, the yield of HNO_2 was 20 μM (Table 2). The slow kinetics and small amplitude in the second stage made the determinations of $[\text{HCrO}_4^-]$ imprecise. For this reason, both chromate ($\epsilon_{350} =$

(26) Neta, P.; Huie, R. E.; Ross, A. B. *J. Phys. Chem. Ref. Data* **1988**, *17*, 1027–1284.

(27) Kimura, M.; Sato, M.; Murase, R.; Tsukahara, K. *Bull. Chem. Soc. Jpn.* **1993**, *66*, 2900–2906.

Table 2. Concentrations (mM) of Products Generated by Steady-State Photolysis of $(\text{H}_2\text{O})_5\text{CrONO}_2^{2+}$

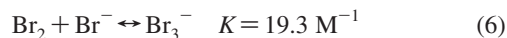
conditions	products	experiment ^a	simulation ^b
Ar	HCrO_4^-	(0.014) ^c	0.011
Ar	HNO_2	0.020	0.018
O_2 , 0.10 M CH_3OH	$\text{Cr}_{\text{aq}}\text{OO}^{2+}$	0.076 ^d	0.088
Ar, 0.050 M Br^-	$\{\text{Br}_2 + \text{Br}_3^-\}$	0.077	0.078
Ar, (0.050 M Br^- + 0.30 M CH_3OH)	$\{\text{Br}_2 + \text{Br}_3^-\}$	0.040	0.040

^a Determined after 60 s of photolysis of 3.0 mM $(\text{H}_2\text{O})_5\text{CrONO}_2^{2+}$ in 0.10 M HClO_4 in argon- or oxygen-saturated solutions at 254 nm. ^b Using $\Delta[(\text{H}_2\text{O})_5\text{CrONO}_2^{2+}] = 0.10$ mM. ^c Determined together with HNO_2 after 17 min of photolysis and normalized to the yield of HNO_2 measured after 60 s of photolysis. ^d Same amount of $\text{Cr}_{\text{aq}}\text{OO}^{2+}$ was obtained with 0.30 M methanol.

2000 $\text{M}^{-1} \text{cm}^{-1}$) and HNO_2 ($\epsilon_{371} = 52.6 \text{ M}^{-1} \text{cm}^{-1}$)²⁸ were determined directly from the spectrum of a sample that was photolyzed for 17 min. The two yields, 60 μM chromate and 100 μM HNO_2 , were close to the expected 1:1.5 ratio. The HCrO_4^- figure in Table 2 was obtained from the experimental $\text{HNO}_2/\text{HCrO}_4^-$ ratio and by normalizing $[\text{HNO}_2]$ to that measured after 60 s. In an independent experiment, it was shown that a solution containing 0.050 mM HNO_2 and 0.030 mM HCrO_4^- in 0.10 M HClO_4 remained unchanged after 10 min of photolysis at 254 nm.

The photolysis of O_2 -saturated solutions of $(\text{H}_2\text{O})_5\text{CrONO}_2^{2+}$ containing 0.10 M CH_3OH yielded 0.076 mM $\text{Cr}_{\text{aq}}\text{OO}^{2+}$, which was identified and quantified on the basis of its characteristic UV spectrum.²⁹ A control experiment, which was identical in every respect except that CH_3OH was omitted, yielded no $\text{Cr}_{\text{aq}}\text{OO}^{2+}$ or other absorbing products.

In a similar experiment, $(\text{H}_2\text{O})_5\text{CrONO}_2^{2+}$ was photolyzed under Ar in the presence of 0.050 M bromide ions. The reaction yielded 38 μM Br_3^- as determined from its UV spectrum.³⁰ Taking into account the equilibrium of eq 6,³⁰ the total bromine yield ($\text{Br}_2 + \text{Br}_3^-$) was 76 μM . The same experiment in the presence of 0.30 M CH_3OH yielded 20 μM Br_3^- (40 μM total bromine).

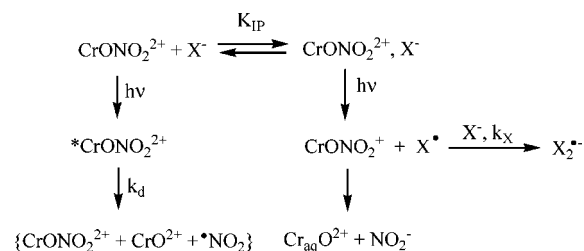


Discussion

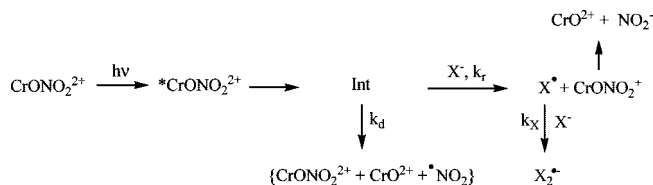
Flash Photolysis. The yields of $\text{X}_2^{\bullet-}$ generated by photochemical oxidation of halide ions with $(\text{H}_2\text{O})_5\text{CrONO}_2^{2+}$ increase with the concentration of X^- (excess reagent) (Figure 3), but the linear plots of k_{obs} against $[\text{X}^-]$ have a zero intercept (Figure 2). Taken together, these findings rule out a standard parallel scheme whereby the photochemically generated X^{\bullet} radicals engage in self-reactions and in the reaction with X^- at similar rates. Such a scheme would require a substantial intercept (corresponding to the self-reaction) in the k_{obs} versus $[\text{X}^-]$ plot and would be additionally unreasonable at the high concentrations of X^- used. The formation of $\text{X}_2^{\bullet-}$ in Figure 2 is so fast that even diffusion-controlled bimolecular reactions of 10–30 μM X^{\bullet} could not contribute measurably to the observed pseudo-first-order rate constants.

The control over the concentration of $\text{X}_2^{\bullet-}$ produced in reaction 3 must lie with the reaction that precedes the formation of $\text{X}_2^{\bullet-}$, that is, with the generation of X^{\bullet} . This step must be exceedingly fast and may involve $(\text{H}_2\text{O})_5\text{CrONO}_2^{2+}, \text{X}^-$ ion

Scheme 1



Scheme 2



pairs and second-sphere photochemistry³¹ followed by the $\text{X}^{\bullet}/\text{X}^-$ reaction as shown in Scheme 1. In this mechanism, the larger concentration of ion pairs is responsible for increased yields of X^{\bullet} at higher $[\text{X}^-]$. The parallel reaction from the non-ion-paired species in Scheme 1 is required by the results of steady-state experiments, as discussed later.

The credibility of the ion-pairing mechanism is weakened by the lack of spectroscopic evidence for ion pairs and by the derived value of K_{IP} that appears too large, as follows. According to Scheme 1, the amount of $\text{X}_2^{\bullet-}$ produced is directly related to the concentration of ion pairs, so that eq 7 applies. Here, Abs_{max} represents the absorbance of $\text{X}_2^{\bullet-}$ at saturation, that is, when $K_{\text{IP}}[\text{X}^-] \gg 1$.

$$\text{Abs} = \frac{\text{Abs}_{\text{max}}}{1 + \frac{1}{K_{\text{IP}}[\text{X}^-]}} \quad (7)$$

This expression is equivalent to that in eq 5, where $a = \text{Abs}_{\text{max}}$, that is, the absorbance at infinitely large $[\text{X}^-]$, and $b = 1/K_{\text{IP}}$, which yields $K_{\text{IP}} \sim 33 \text{ M}^{-1}$ for both Br^- and I^- . This value is significantly greater than our predicted K_{IP} of $< 1 \text{ M}^{-1}$. We arrived at this estimate on the basis of the available data for $\text{Cr}_{\text{aq}}^{3+}$, which has $K_{\text{IP}} = 4 \text{ M}^{-1}$ for $\text{X}^- = \text{Cl}^-$, and much less for bromide and iodide.³² Ion pairing with the 2+ charged nitratochromium complex should be even weaker.

Our experimental observations can also be explained by a mechanism featuring reduction of an excited state (or, more likely, an intermediate derived from it) by X^- in parallel with the self-decay of the intermediate. Both of these reactions must take place prior to the observed $\text{X}^{\bullet}/\text{X}^-$ reaction (Scheme 2).

The proportion of the intermediate that yields $\text{X}_2^{\bullet-}$ is given by the expression in eq 8, which is also equivalent to eq 5 with $b = k_{\text{d}}/k_{\text{r}}$. From $\text{Abs}_{\text{max}} = 0.13$, we calculate $[\text{X}_2^{\bullet-}]_{\text{max}} = 4 \times 10^{-5} \text{ M}$. Taking into account that k_{r} and k_{X} are nearly diffusion-controlled, and that k_{r} must be larger than k_{X} if the two steps are reasonably separated in time as required by the experiment, we estimate $k_{\text{r}} \leq 3 \times 10^{10} \text{ M}^{-1} \text{ s}^{-1}$. The larger rate constant

(28) Pestovsky, O.; Bakac, A. *J. Am. Chem. Soc.* **2002**, *124*, 1698–1703.

(29) Bakac, A. *Adv. Inorg. Chem.* **2004**, *55*, 1–59.

(30) Beckwith, R. C.; Wang, T. X.; Margerum, D. W. *Inorg. Chem.* **1996**, *35*, 995–1000.

(31) Balzani, V.; Sabbatini, N. *Chem. Rev.* **1986**, *86*, 319–337.

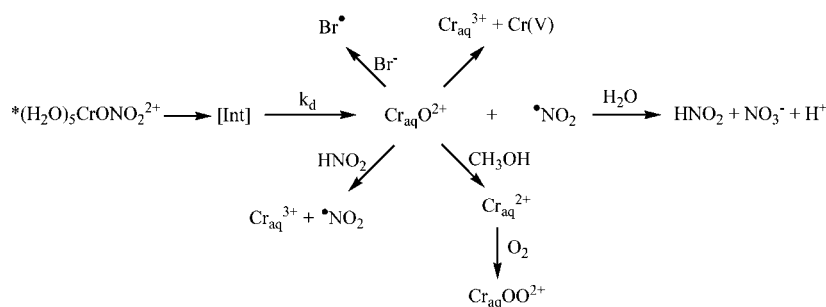
(32) Wrona, P. K. *Inorg. Chem.* **1984**, *23*, 1558–1562.

(33) Jiang, P. Y.; Katsumura, Y.; Ishiguro, K.; Yoshida, Y. *Inorg. Chem.* **1992**, *31*, 5135–5136.

(34) Stanbury, D. M. *Adv. Inorg. Chem.* **1989**, *33*, 69–138.

(35) Bakac, A. *Prog. Inorg. Chem.* **1995**, *43*, 267–351.

Scheme 3



for this step may be justified by the favorable electrostatics. The ratio $k_d/k_r = 0.03$ then provides an estimate for the lifetime of the intermediate, $\tau \geq 1$ ns ($k_d \leq 10^9$ s $^{-1}$).

$$\frac{[X_2^{\bullet-}]}{[Int]} = \frac{Abs}{Abs_{max}} = \frac{1}{1 + \frac{k_d}{k_r[X^-]}} \quad (8)$$

The major difference between the two mechanisms is the source of the increasing yields of X_2 with increasing $[X^-]$ in laser flash photolysis experiments, that is, the concentration of ion pairs versus competition between the decay and reduction of the oxidizing intermediate. Common to both schemes is the requirement that the halogen atom generating entity be a powerful oxidant so that it can react with all three halides at diffusion-controlled rates. Regardless of the nature of the excited state initially populated (intraligand $\pi\pi^*$, $n\pi^*$, or LMCT), the most reasonable oxidant is either a charge-separated intermediate $\{Cr^{II}, ONO_2^{\bullet}\}^{2+}$ or free nitrate radical derived from it. The radical has a reduction potential of 2.7 V 33 and is thermodynamically capable of oxidizing even Cl^- ($E = 2.4$ V). 34

It is not possible to determine with certainty whether the reacting halide ion was part of an ion pair, as shown in Scheme 1, or a freely diffusing species, but the latter seems more plausible in view of the unreasonably large value of K_{IP} that would be required to explain the data and the lack of spectroscopic evidence for ion pairs.

Steady-State Photolysis. The products observed after 60 s of photolysis are shown in Table 2. The most distinguishing features are as follows. (1) Large amounts of $Cr_{aq}OO^{2+}$ were generated when both oxygen and methanol were present, but no $Cr_{aq}OO^{2+}$ was observed in the absence of methanol. (2) Photolysis under argon in the presence of bromide generated bromine. (3) The amounts of bromine and $Cr_{aq}OO^{2+}$, obtained in separate experiments and with different additives (Br^- vs O_2/CH_3OH), are approximately the same. (4) The yield of bromine decreased by about 50% if both Br^- (50 mM) and methanol (0.30 M) were present in the photolyzing solution.

The fact that methanol did not completely block the formation of bromine requires that more than one reaction is responsible for its generation. This observation is consistent with the proposed mechanism (Scheme 2), where both the fast reduction of the intermediate with Br^- (k_r) and slower oxidation of Br^- by $Cr_{aq}O^{2+}$ formed in k_f and k_d steps will lead to Br_2 .

The formation of $Cr_{aq}OO^{2+}$ in the presence of O_2 strongly implicates the Cr_{aq}^{2+}/O_2 reaction. The requirement for CH_3OH , however, shows that bulk Cr_{aq}^{2+} is generated only after the primary photolysis step, most likely by the reduction of $Cr_{aq}O^{2+}$ with CH_3OH , a known one-step two-electron process. 35 Also, the observation that the final concentrations of $Cr_{aq}OO^{2+}$ and

Table 3. Reactions Used in Kinetic Simulations a

reaction	$k/M^{-1} s^{-1}$ or s^{-1}	reference
$Int \rightarrow Cr_{aq}O^{2+} + NO_2$	1×10^9	this work
$2 Cr_{aq}O^{2+} \rightarrow Cr^{3+} + Cr(V)$	260	37
$Cr_{aq}O^{2+} + NO_2 \rightarrow Cr^{3+} + NO_2$	950	39
$2 NO_2 \rightarrow NO_2^- + NO_3^-$	5×10^8	38
$CrO^{2+} + CH_3OH \rightarrow Cr^{2+} + CH_2O$	52	35
$Cr^{2+} + O_2 \rightarrow CrOO^{2+}$	1.6×10^8	41
$Cr^{2+} + CrOO^{2+} \rightarrow CrO^{2+}$	5×10^8	b
$Int + Br^- \rightarrow Br + CrO^{2+} + NO_2^-$	3×10^{10}	this work
$Br + Br^- \rightarrow Br_2^-$	1.4×10^{10}	this work
$2 Br_2^- \rightarrow Br_2 + 2Br^-$	4×10^9	26
$CrO^{2+} + Br^- \rightarrow Cr^{3+} + Br$	61	36
$2 Cr(V) \rightarrow Cr(VI) + CrO^{2+}$	1×10^5	c

a Using the mechanism in Scheme 2. Numerically identical results are obtained with the ion-pairing Scheme 1 and $K_{IP} = 33$ M $^{-1}$. b Estimated from $k = 8 \times 10^8$ M $^{-1}$ s $^{-1}$ at 1.0 M ionic strength. 35 c Estimated from data at higher pH in ref 40.

Br_2 in separate experiments (see Table 2) are comparable suggests that in both cases the intermediates are converted to products quantitatively. Even though the yields of $Br_2^{\bullet-}$, and thus Br_2 , on short, flash photolysis time scales vary with $[Br^-]$ (Figure 3), the final yields are quantitative because the slow subsequent steps also generate Br_2 .

All the observations suggest that the portion of the intermediate that was not scavenged by halide ions reacted by $CrO-NO_2$ bond cleavage to generate $Cr_{aq}O^{2+}$ and $\bullet NO_2$, which led to the final observed products, as shown in Scheme 3.

$Cr_{aq}O^{2+}$ will react with CH_3OH to give Cr_{aq}^{2+} and formaldehyde ($k/M^{-1} s^{-1} = 52$) 35 or with Br^- to give Cr_{aq}^{3+} and Br^{\bullet} ($k/M^{-1} s^{-1} = 608 [H^+]$). 36 The disproportionation ($k/M^{-1} s^{-1} = 38.8/[H^+]$) 37 generates Cr(III) and Cr(V). The most likely fate of nitrogen dioxide is disproportionation to nitrate and nitrite, $k = 4.5 \times 10^8$ M $^{-1}$ s $^{-1}$. 38 The latter will also react with $Cr_{aq}O^{2+}$ ($k = 950$ M $^{-1}$ s $^{-1}$ in 0.10 M $HClO_4$) 39 and regenerate $\bullet NO_2$. A reaction scheme incorporating these steps, as well as the disproportionation of Cr(V), 40 was used to simulate the photochemical reaction. The concentration of $(H_2O)_5CrONO_2^{2+}$ that was consumed during the photolysis was estimated as 0.10 mM, but the calculated product yields (in %) were the same regardless of the initial concentration of the excited state. The complete set of equations used in the simulation is given in Table 3.

The results in Table 2 show good agreement between the experimental and calculated yields for all the products. Espe-

(36) Hung, M.; Bakac, A. *Inorg. Chem.* **2005**, *44*, 9293–9298.

(37) Nemes, A.; Bakac, A. *Inorg. Chem.* **2001**, *40*, 2720–2724.

(38) Stedman, G. *Adv. Inorg. Chem. Radiochem.* **1979**, *22*, 113–170.

(39) Pestovsky, O.; Bakac, A. *J. Mol. Catal. A* **2003**, *200*, 21–29.

(40) Buxton, G. V.; Djouider, F. *J. Chem. Soc., Faraday Trans.* **1996**, *92*, 4173–4176.

cially convincing is the role of various additives (bromide, methanol, and oxygen), all of which exhibit the precise effect expected for a scheme having $\text{Cr}_{\text{aq}}\text{O}^{2+}$ and $\cdot\text{NO}_2$ as major intermediates. The latter influences the reaction only indirectly by generating $\text{HNO}_2/\text{NO}_2^-$ which reduces $\text{Cr}_{\text{aq}}\text{O}^{2+}$ and, perhaps, $\text{Cr}(\text{V})$.

We estimated the disproportionation rate constant for $\text{Cr}(\text{V})$ as $10^5 \text{ M}^{-1} \text{ s}^{-1}$ based on the reported data at higher pH.⁴⁰ No other reactions of $\text{Cr}(\text{V})$ applicable to our system are known, but one might expect the oxidation of nitrite and reduction of $\text{Cr}_{\text{aq}}\text{O}^{2+}$ to be important under our conditions. When such reactions are added to the simulated scheme, the yields of chromate decrease somewhat, but the absence of experimental data limits the value of this exercise.

We cannot exclude the possibility that the cleavage of the N–O bond to generate $\text{Cr}_{\text{aq}}\text{O}^{2+}$ and $\cdot\text{NO}_2$ in Schemes 1 and 2 is preceded by isomerization of $(\text{H}_2\text{O})_5\text{CrONO}_2^{2+}$ to the peroxyxynitrite complex $(\text{H}_2\text{O})_5\text{CrOONO}^{2+}$. Such a path would be analogous to the known fast (2 ps) isomerization of photoexcited nitrate anion^{5,42} and also consistent with the known²¹ fast decomposition of $(\text{H}_2\text{O})_5\text{CrOONO}^{2+}$ to $\text{Cr}_{\text{aq}}\text{O}^{2+}$ and $\cdot\text{NO}_2$.²¹ However, the isomerization could be, at best, a competing pathway. It cannot precede the oxidation of halides in the flash photolysis experiments because neither peroxyxynitrite anion nor peroxyxynitrite radical have the potential to oxidize all three halide ions to halogen atoms.⁴³

In a related study of the 254 nm photolysis of $\text{Cr}(\text{NH}_3)_5\text{Cl}^{2+}$ and similar complexes, chromate was observed among the reaction products when either O_2 (0.1–1 mM) or nitrate (0.10 M) was present.¹⁷ Ion pairing and a reactive LMCT state were proposed to explain the nitrate results. We note that free nitrate also absorbed significant amounts of light in those experiments.¹⁷ It is now known⁵ that $\text{HOONO}/\text{OONO}^-$ had to be produced, so that this and other intermediates probably also played a role in product formation.

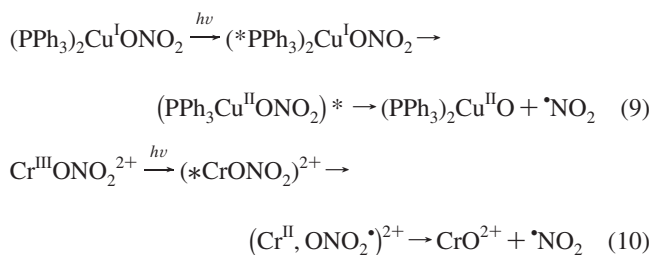
Conclusions

Laser flash photolysis of $\text{Cr}_{\text{aq}}\text{ONO}_2^{2+}$ generates a strongly oxidizing intermediate that is capable of oxidizing halides to halogen atoms on nanosecond time scales. In a parallel channel, and in the absence of added substrates, the intermediate decays to $\text{Cr}^{\text{IV}}_{\text{aq}}\text{O}^{2+}$ and NO_2 . The former was identified by its signature reaction with $\text{CH}_3\text{OH}/\text{O}_2$ to produce $\text{Cr}_{\text{aq}}\text{OO}^{2+}$ and by its slow reaction with Br^- .

The initial excitation of $\text{Cr}_{\text{aq}}\text{ONO}_2^{2+}$ is suggested to generate a LMCT excited state to account for the oxidizing power of

the species—charge-separated intermediate or free nitrate radical—that oxidizes halide ions prior to the X^*/X^- reaction observed in laser flash photolysis experiments. In an earlier study of the photochemistry of $(\text{PPh}_3)_2\text{Cu}^{\text{I}}\text{NO}_3$,⁸ it was suggested that a MLCT excited state was involved, and that it was responsible for the observed formation of $\text{Cu}(\text{II})$ and (presumably) $\cdot\text{NO}_2$, followed by thermal chemistry between $\cdot\text{NO}_2$ and PPh_3 . In the work with the nitrate complexes of Mn and Fe porphyrins, it was also shown that M^{IV} species were generated.⁹ Both the copper and metal porphyrin studies utilized only steady-state photolysis so that, unfortunately, no information on short-lived intermediates was obtained, and only a luminescence spectrum of $(\text{PPh}_3)_2\text{Cu}^{\text{I}}\text{NO}_3$ was reported.

It is interesting to note that, in all the cases examined, the ultimate result was the oxidation of the metal regardless of the (proposed) nature of the excited state (i.e., LMCT or MLCT). This outcome is determined initially when the excited state is MLCT as in the copper example,⁸ eq 9, or after the initial charge separation and oxygen atom transfer from coordinated nitrate radical to the reduced metal when the excited state is LMCT, as in the $\text{Cr}_{\text{aq}}\text{ONO}_2^{2+}$ case of eq 10. The generation of a MLCT excited state in the copper example⁸ of eq 9 is a reasonable proposal, although the experimental support is still lacking. The LMCT excited state in the present work draws strong support from the oxidizing power exhibited by the system at short times. The rapid oxidation of halides in laser photolysis experiments is consistent with an intermediate resembling nitrate radicals²⁶ and clearly inconsistent with species such as $\text{Cr}_{\text{aq}}\text{O}^{2+}$ and/or $\cdot\text{NO}_2$ which are produced only later and are involved in slow oxidations of substrates such as Br^- or CH_3OH . Thus, despite the large positive reduction potential³³ of NO_3 radicals, the initial photochemical step for $\text{Cr}_{\text{aq}}\text{ONO}_2^{2+}$ is similar to that observed with complexes of the more easily oxidizable ligands, such as NO, superoxide, or alkyl. In the $\text{Cr}_{\text{aq}}\text{ONO}_2^{2+}$ case, however, the two high energy products, $\{\text{Cr}_{\text{aq}}^{2+}, \cdot\text{NO}_3\}$, engage in rapid O-atom transfer to yield a lower-energy pair, $\text{Cr}_{\text{aq}}\text{O}^{2+}$ and $\cdot\text{NO}_2$.



Acknowledgment. This work was supported by a grant from National Science Foundation, CHE 0602183. Some of the work was conducted with the use of facilities at the Ames Laboratory.

JA8000453

(41) Sellers, R. M.; Simic, M. G. *J. Am. Chem. Soc.* **1976**, *98*, 6145–6150.

(42) Goldstein, S.; Rabani, J. *J. Am. Chem. Soc.* **2007**, *129*, 10597–10601.

(43) Nauser, T.; Merkofer, M.; Kissner, R.; Koppenol, W. H. *Chem. Res. Toxicol.* **2001**, *14*, 348–350.